

A Computationally Efficient and Reliable Bond Order Measure

Raúl Mera-Adasme,^{*,†,‡} Fernando Mendizábal,^{†,⊥} Claudio Olea-Azar,[‡] Sebastián Miranda-Rojas,^{†,‡} and Patricio Fuentealba^{⊥,§}

[†]Department of Chemistry, Faculty of Sciences, Universidad de Chile, Las Palmeras 3425, Ñuñoa, Santiago, Chile

[‡]Department of Analytic and Inorganic Chemistry, Faculty of Chemical and Pharmaceutical Sciences, Universidad de Chile, Independencia, Santiago, Chile

[⊥]Center for the Development of Nanoscience and Nanotechnology, Cedenna, Santiago, Chile

[§]Department of Physics, Faculty of Sciences, Universidad de Chile, Ñuñoa, Santiago, Chile

ABSTRACT:

$$\eta_{i,j}^{norm} = \frac{1}{\sqrt{1 + \sum_j \eta_{i,j}^2}} \frac{\langle \phi_i^{(0)} | \mathcal{F} | \phi_j^{(0)} \rangle}{\epsilon_j - \epsilon_i}$$

Bond order indexes are useful measures that connect quantum mechanical results with chemical understanding. One of these measures, the natural bond order index, based on the natural resonance theory procedure and part of the natural bond orbital analysis tools, has been proved to yield reliable results for many systems. The procedure's computational requirements, nevertheless, scales so highly with the number of functions in the basis set and the delocalization of the system, that the calculation of this bond order is limited to small or medium size molecules. We present in this work a bond order index, the first order perturbation theory bond order (fopBO), which is based on and strongly connected to the natural bond orbital analysis tools. We present the methodology for the calculation of the fopBO index and a number of test calculations that shows that it is as reliable as the natural bond orbital index, with the same weak sensitivity to variations among commonly used basis sets and, as opposed to the natural bond order index, suitable for the study of large systems, such as most of those of biological interest.

INTRODUCTION

In the theoretical study of molecules, it is helpful to have an index that connects quantum mechanical results with the common chemical intuition, facilitating the extraction of chemical knowledge from calculated results.^{1–5} Among the measures that can be used in that way are the bond order indexes.

Different attempts to define quantum mechanical bond order measures that agree with the common chemical knowledge have been presented over the years (see the work by Mayer for a review⁶). One of them, the natural bond order,⁷ is based on the widely used NBO analysis.⁵

This bond order has been proven to be reliable, weakly sensitive to variations among currently used basis sets and in good agreement with general chemical intuition. As a short description of the procedure, the bond order is calculated based on the natural resonance theory, or NRT. For a given chemical system, the second order reduced density matrix is expressed as the variationally best linear combination of density matrices corresponding to idealized “resonant” Lewis structures for the system. For a given pair of atoms, the bond order is calculated as the average bond order along all those idealized structures, each bond order weighted by the coefficient of the corresponding density matrix in the linear combination.⁷

While this natural resonance theory-based bond order index is resting on the strong NBO foundations, and performs well for

small systems,⁷ its use in big systems, like the ones which computational biochemists are commonly dealing with, is limited. Because of the extremely large amount of terms needed to express a system with a large number of electrons, as is common in biologically relevant systems, as a linear combination of localized density matrices, the index becomes difficult to obtain for those cases. The scaling of memory usage by the NRT procedure is difficult to assess because of its dependence not only on the number of electrons but also on the number of resonance structures needed to represent of the system.

The particular case of the protein copper zinc superoxide dismutase (Cu,Zn SOD) is instructive. This protein, crystallized at high resolution,^{8,9} is part of the antioxidant machinery of the cell and many mutations on its sequence have been linked to the amyotrophic lateral sclerosis neurological disorder.¹⁰ Although it is biologically important to describe the electronic structure of the active site of the enzyme, this active site is too large and delocalized to be easily expressed as a linear combination of localized Lewis structures, especially when a large basis set is used.

To overcome the difficulties of calculating the NBO bond order index for such biologically relevant molecules, we present

Received: August 9, 2010

Revised: January 26, 2011

Published: April 06, 2011

in this work the fopBO (first order perturbation theory bond order), a bond order measure based on the NBO framework and easily interpretable based on the results from the different NBO analysis tools.¹¹ This bond order measure is based on the NBO results for a single structure; hence, a NRT calculation is not required. Since most of the numerical calculations required for obtaining the fopBO index are routinely performed in the default NBO run, the fopBO is readily calculated from a NBO output.

In the following sections, we give details on the methodology of the fopBO measure. Then, we present exhaustive evaluation of its results for different systems, from simple cases like hydrocarbons, for which bond orders can be easily assigned on the basis of general chemical intuition, to complex, biologically relevant systems like hydrogen bonds and metal–ligand interactions in inorganic complexes.

THEORETICAL BASIS

The first order perturbation theory bond order (fopBO) is based in the natural bond orbital⁵ framework. For calculating it, an NBO analysis output¹² is required.

The procedure for calculation of the fopBO index uses the Lewis structure suggested by NBO⁴ for the system as an “unperturbed” localized starting point. To each bonding orbital found by NBO¹² an occupation of 1 or 2 is assigned, for unrestricted and restricted wave functions, respectively, whereas to all antibonding orbitals an occupation of 0 is assigned. This unperturbed localized structure is corrected by adding delocalization with uncoupled first order perturbation theory. A similar, but simplified procedure is used in the textbook by Weinhold and Landis¹¹ for the calculation of the charge transferred in a donor–acceptor interaction. Note that the uncoupled treatment has been successfully used as a part of the standard NBO analysis package¹³ For examples, see the review by Reed et al.¹⁴

To illustrate the procedure, let us assume a restricted wave function. The unrestricted case can be easily considered, as shown below. For a pair of atoms A and B, the first order perturbation correction for the interaction between an occupied orbital from atom A, $\phi_i^{(0)}$ and a set of empty orbitals from other atoms $\phi_j^{(0)}$ would be:

$$\phi_i^{(1)} = \phi_i^{(0)} + \sum_j \eta_{i,j} \phi_j^{(0)} \quad (1)$$

with the coefficients $\eta_{i,j}$ related to the Fock matrix and to the energy difference between the orbitals ϕ_i and ϕ_j

$$\eta_{i,j} = \frac{\langle \phi_i^{(0)} | \mathcal{F} | \phi_j^{(0)} \rangle}{\epsilon_j - \epsilon_i} \quad (2)$$

This gives for the normalized perturbed orbital

$$\phi_i^{(1)norm} = \frac{1}{\sqrt{1 + \sum_j \eta_{i,j}^2}} (\phi_i^{(0)} + \sum_j \eta_{i,j} \phi_j^{(0)}) \quad (3)$$

and the normalized coefficients

$$\eta_{i,j}^{norm} = \frac{1}{\sqrt{1 + \sum_j \eta_{i,j}^2}} \frac{\langle \phi_i^{(0)} | \mathcal{F} | \phi_j^{(0)} \rangle}{\epsilon_j - \epsilon_i} \quad (4)$$

Consider a bond order of 1 to occur between atoms A and B when the occupied orbital ϕ_i from A and the empty orbital ϕ_j

from B are combined to an extent that the charge of two electrons are transferred to orbital ϕ_j (for instance, in the opposite case, for a single bond to be broken, two electrons need to be transferred to the corresponding antibonding orbital). With that consideration we can define the contribution to the bond order between atoms A and B arising from the interaction between an occupied orbital ϕ_i from atom A and an unoccupied orbital ϕ_j from atom B as half of the charge transferred from the occupied orbital ϕ_i to an empty orbital ϕ_j , which has a maximum of 2 in the restricted case.

$$BO_{i,j}^{AB} = 0.5 \times CT \approx |\eta_{i,j}^{norm}|^2 \quad (5)$$

Thus, for the calculation of the total bond order, interactions between all occupied orbitals from atom A $\{\phi_i\}$ with all empty orbitals from atom B $\{\phi_j\}$, and *vice versa* are considered and summed up. Donations from any orbital ϕ_k from any atom C to an antibonding orbital between atoms A and B (which is empty at the unperturbed level) are calculated and subtracted from the total bond order. Interactions between a fully occupied bonding orbital between atoms A and B and any given empty orbital, are also subtracted.

The relevant Fock matrix elements, i.e., those with delocalization energy at second order perturbation theory of 0.5 kcal/mol by default, and the corresponding orbital’s energy differences are calculated by the NBO program, and those results are transferred from the NBO output to the calculation of the fopBO index. Because of that, the calculation of this first order perturbation bond order requires very little computational effort, even for systems with a large number of atoms.

For the case of unrestricted determinants, the calculation is the same, but to the initial unperturbed bonding orbitals and lone pair orbitals, occupation numbers of 1 are assigned. Each contribution to the bond order from the interaction of two orbitals is also multiplied by 0.5.

Since, as detailed above, the fopBO method is based on perturbation theory, is especially adequate to measure the effect of small effects on the initial, unperturbed structure. These effects, like weak interactions (such as hydrogen bonds) or hyperconjugation and other substituent effects on a particular bond, are most often the type of interaction of interest when studying biological systems. Systems for which there are few and strong deviations from the initial structure are not properly treated by low order perturbation theory.

COMPUTATIONAL DETAILS

Structures, either those generated *de novo* or those derived from crystallographic data were subject to optimization with appropriate constrains, discussed below, for each structure. They were preoptimized at the semiempirical PM6¹⁵ level of theory with the program MOPAC2009¹⁶ and then optimized with the BP86^{17,18} density functional and Stuttgart effective core potentials (ECP),¹⁹ with the corresponding basis set plus one extra d-type polarization function for carbon, nitrogen and oxygen ($\alpha_N = 0.864, \alpha_C = 0.6, \alpha_O = 1.154$)²⁰ The DFT geometry optimizations were carried out with the program TURBOMOLE V5.9²¹ and the resolution of identity (RI) approximation.^{22–26}

Structures for butane, 2-butene and 2-butyne were created *de novo* with the Avogadro molecular editor.²⁷ The optimization protocol was applied to them without constrains.

Structures for the zinc complexes were derived from the crystallographic structure of the oxidized bovine Cu,Zn SOD resolved at 1.65 Å,⁸ by manually adding or removing atoms to

Table 1. NRT-Based and fopBO Bond Order Indexes for C_2-C_3 Bond in Butane, *trans*-2-Butene and 2-Butyne

basis	butane		<i>trans</i> -2-butene		2-butyne	
	NRT	fopBO	NRT	fopBO	NRT	fopBO
3-21G	1.009	1.000	1.954	1.967	2.883	2.911
6-31G*	1.010	1.004	1.954	1.969	2.890	2.916
6-311G**++	1.013	1.007	1.952	1.970	2.880	2.906
Stuttgart ECP	1.013	1.007	1.952	1.967	2.881	2.907
def2-TZVPP	1.011	1.006	1.953	1.972	2.879	2.909

obtain the final complexes, which were optimized with the protocol detailed above and without any constraint.

The structure of the reduced active site of Cu,Zn SOD (91 atoms) was derived from the crystallographic structure at 1.15 Å of resolution.⁹ Hydrogens were added manually to the reduced model. The resulting structure was optimized with the protocol described above, keeping fixed all atoms except hydrogens.

All single point calculations were performed at the B3LYP^{28–31} density functional level of theory with the PC-GAMESS/Firefly program,³² partially based on the GAMESS(US) program.³³ For butane, 2-butene, 2-butyne and butadiene, single points were carried out with the following basis sets: 3-21G,³⁴ 6-31G*, 6-311G**++,³⁵ the Stuttgart ECPs plus polarization functions, as described in the “structures preparation” and the all electron def2-TZVPP basis set.³⁶ For the reduced active site of 91 atoms from Cu,Zn SOD, single point calculations were performed with two different basis sets: First, Stuttgart-ECP plus an extra polarization function for carbon, nitrogen and oxygen, and second, the def2-TZVPP basis set for all atoms except carbon, zinc and copper, which were treated with Stuttgart-ECP plus the mentioned polarization basis for carbon. For the zinc complexes and the reduced hydrogen-bonded systems, single point calculations were carried out with Stuttgart-ECP plus the above-mentioned polarization functions and with the def2-TZVPP basis set.

NBO entries were produced by the NBO¹² code incorporated in the PC-GAMESS/Firefly program. Complete analyses were performed with the standalone NBO program. Natural bond order was obtained from NRT⁷ calculations when possible (see the Results and Discussion). Total valences were calculated by adding the bond orders for a given atom with all atoms interacting with it, i.e., with bond order index > 0, bond orders among atoms with themselves, which are not necessarily equal to zero in the natural bond order index, were not considered.

Figures were prepared with PyMOL³⁷ and gOpenMol^{38,39}

RESULTS AND DISCUSSION

In order to test the behavior of the first order perturbation theory bond order index (fopBO), we chose molecules representative of different bonding situations. In these trials, we compared the performance of the fopBO with that of the natural bond order index, which is based on the natural resonance theory.⁷ We tested both indexes for stability on different basis sets, and for agreement with the general chemical knowledge. Since a previous study has shown that the natural bond order performs significantly better than other, traditionally used bond order indexes, we saw no need for including these other bond order measures in this study.

Localized Single, Double, and Triple Carbon–Carbon Bonds. In Table 1, the NRT-based and the fopBO bond orders

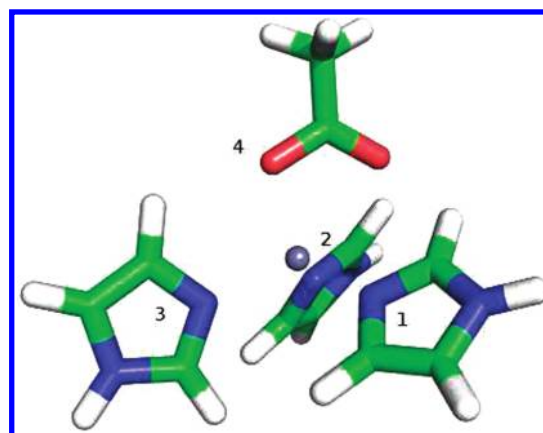


Figure 1. Optimized geometry for the compound triimidazoleacetozinc(II). Numbers are arbitrarily assigned to ligands. The zinc radius is reduced for clarity.

indexes for the C_3-C_4 bonds in butane, *trans*-2-butene, and 2-butyne, respectively, calculated with several different basis sets are shown. As can be seen, both bond order indexes yield very similar values for these systems. Both bond order indexes are reasonably independent of the basis set (the NRT-based is slightly more stable) and they produce values that are in line with those expected by chemical intuition.

Zinc Complexes. In order to assess the performance of the NRT-based and the fopBO bond order indexes in inorganic compounds, we optimized the geometry for triimidazoleacetozinc(II), a system of biological interest due to its relation to the active site of the Cu,Zn superoxide dismutase enzyme. The result is shown in Figure 1. For this system we tried to analyze the metal–ligand interactions with both bond order indexes. Because of the high memory demand of the NRT procedure for large, highly delocalized systems, it was not possible for us to perform the NRT analysis.

To compare the results from both bond order indexes, we reduced the system to triaminoacetozinc(II) whose optimized geometry is shown in Figure 2. For the NRT measure, it was necessary to manually include the relevant resonance structures in the NBO input. The results for both molecules (fopBO only for tetraimidazoleacetozinc(II) and both of the indexes for tetraaminoacetozinc(II)) are presented in Table 2 and Table 3.

Table 2 shows that both indexes display reasonable values for the metal–ligand interactions. fopBO treatment seems to be more stable upon basis set change and gives more similar results for the three different Zn–N interactions than NRT. On the other hand, the NRT treatment gives a better resolution between the Zn–N and the Zn–O interactions. Even though the difference in distances between these two types of bonds is not big (average Zn–N distance for triaminoacetozinc(II), 2.0954 Å, Zn–O distance for the same molecule, 1.9709 Å), some difference in the bond orders is expected. The reason why fopBO delivers a very similar bond order for the Zn–N and the Zn–O interactions seems to be that fopBO assigns a significant bond order for the interaction between Zn and the other carboxylate oxygen (fopBO: 0.014), which is not considered to interact with the metal ion in the NRT description (natural bond order: 0.002). The difference could be also related to the larger ionicity of the Zn–O interaction compared to that of the Zn–N interaction as discussed below for pentaaminoacetozinc(II). It is not clear from geometry analysis

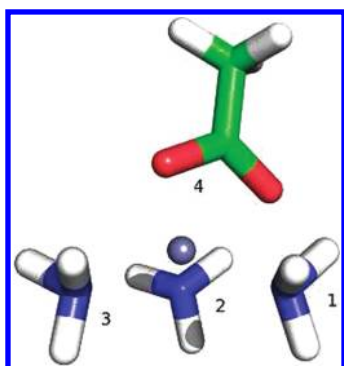


Figure 2. Optimized geometry for the compound triaminoacetozinc(II). Numbers are arbitrarily assigned to ligands. The zinc radius is reduced for clarity.

Table 2. NRT-Based and fopBO Bond Orders for Metal–Ligand Interactions in Triaminoacetozinc(II)^a

basis set	N ₁		N ₂		N ₃		O ₄	
	NRT	fopBO	NRT	fopBO	NRT	fopBO	NRT	fopBO
Stuttgart	0.204	0.122	0.168	0.122	0.239	0.124	0.367	0.131
def2-TZVPP	0.174	0.116	0.112	0.114	0.239	0.116	0.369	0.125

^aNumbering are those used in Figure 2.

Table 3. fopBO Bond Orders for Zinc–Ligand Interactions in Triimidazoleacetozinc(II)^a

basis set	N ₁	N ₂	N ₃	O ₄
Stuttgart	0.105	0.105	0.092	0.100
def2-TZVPP	0.084	0.083	0.074	0.094

^aNumbering are same as used in Figure 1.

which of these descriptions is more correct, but it is clear that there are significant differences between both of the Zn–O distances (Zn–O₁, 1.97 Å; Zn–O₂, 2.48). This suggests that one of the interactions is considerably stronger than the others, in agreement with NRT and fopBO data.

In Table 3, similar values for the fopBO measures can be seen, though some decrease in the bond order is observed. This is reasonable since in the ammonia molecule all valence electron density is in the σ system and can contribute to bonding with the metal, while in the imidazole system, a part of the electron density is associated with the π system in the ring, which does not contribute significantly to bonding. In the case of the acetate group, the observed difference is probably due to electrostatic repulsion among the ligands and the π system of the imidazole groups. It is interesting to note that the difference just discussed is strongly dependent on the basis set, which is expected in cases of weak interactions which are not well described by small basis sets. The same applies to the bond order difference between Zn–O and Zn–N.

In order to assess the effect of adding additional ligands to Zn complexes, we obtained and analyzed an optimized geometry of a six-coordinate system, pentaaminoacetozinc(II), which is shown in Figure 3. Amines were used instead of the more biologically relevant imidazole to access the NRT-based bond order indexes. In order to avoid NRT memory constraints, calculations were performed only with Stuttgart ECP basis. Again, the NRT results

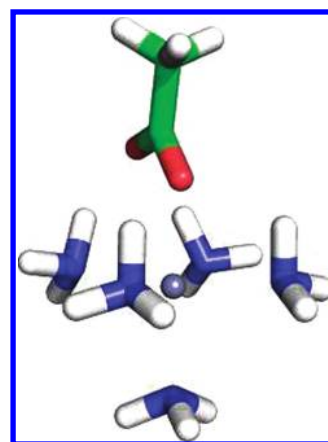


Figure 3. Optimized geometry for the compound pentaaminoacetozinc(II). Zinc radius is reduced for clarity.

Table 4. NRT-Based and fopBO Bond Orders Indexes for Metal–Ligand Interactions in Pentaaminoacetozinc(II)^a

basis set	Zn–N(average)		Zn–O	
	NRT	fopBO	NRT	fopBO
Stuttgart	0.100	0.099	0.368	0.106

^aZn–N bonds are averaged for clarity.

were obtained by manually adding the relevant resonance structures to the NBO input.

As discussed by Weinhold and Landis,¹¹ Zn(II) uses its empty 4s orbital to accept charges from donors. Thus, all donors compete for this only acceptor and one would expect a decrease in the bond orders when additional ligands are added. This is observed in both the NRT-based and the fopBO measures when comparing the indexes for triaminoacetozinc(II) from Table 2 with the average values for pentaaminoacetozinc(II) in Table 4. There are significant differences between these two measures when comparing the values for the Zn–O interaction. The NRT value is even larger than the value for triaminoacetozinc(II), while the fopBO gives a value that is very similar to the one for Zn–N interactions. Although both results appear counterintuitive, they can be explained if one considers that the NRT-based bond order includes ionic interactions⁷ while the fopBO indicator measures orbital interactions exclusively. Since the Zn–O interaction is expected to be more ionic than the Zn–N interaction, the results delivered by both measures are reasonable and complementary. Notice that due to the use of completely different procedures in both measures, the “covalent” part of the Natural bond order (0.029) is not equivalent to the fopBO measure (0.106).

From the examples given above, it can be concluded that both bond orders measures deliver reasonable values for metal–ligand interactions in zinc complexes, and in some cases, it is particularly enlightening to compare the results for both measures. For large systems, the fopBO measure is the only available option, due to the memory requirements of the NRT procedure. Moreover, fopBO can be useful to determine in which cases the reference structures for the NRT analysis have to be manually added to the NBO input, and it can also be used to determine such structures.

Hydrogen Bonds. *β -Hydroxyacrolein.* In order to compare the performances of the fopBO and NRT bond order measures in

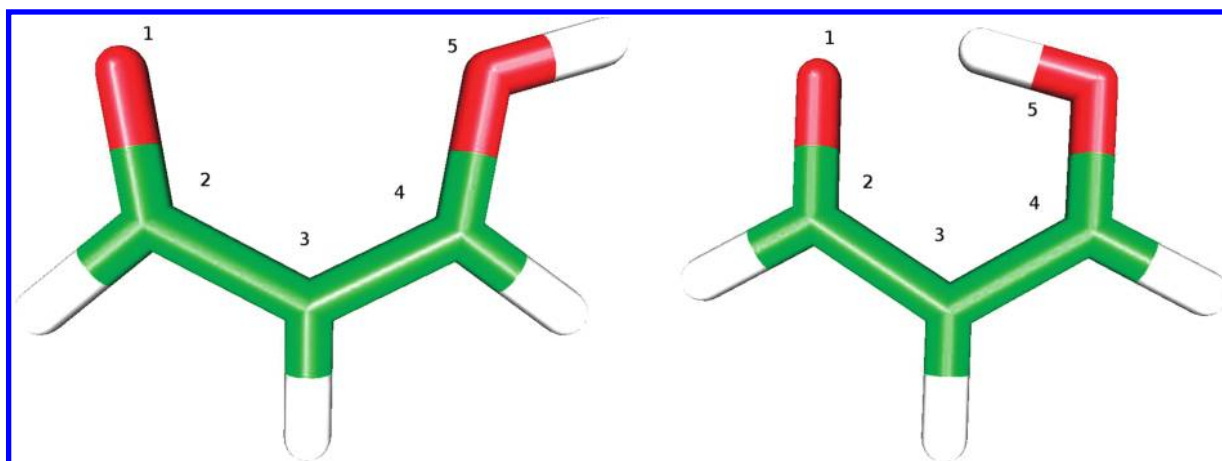


Figure 4. Optimized geometries for open (left) and closed conformations for β -hydroxyacrolein.

describing hydrogen bonds, which are of unquestionable chemical and biological interest, we used two conformations of the molecule β -hydroxyacrolein, systems previously used to illustrate the performance of the NRT measure in these interactions.¹¹ Both of the conformations, which we will call here “open” and “closed” are shown in Figure 4. From this figure, it can be seen that only the closed conformation presents an hydrogen bond between the enolic hydrogen and oxygen 1 (the arbitrary numbering convention is also displayed in Figure 4). This hydrogen bond should result in two resonance structures for the closed conformation, causing the double bond, localized between atoms 3 and 4 in the open structure, delocalize partially toward atoms 2 and 3 in the closed one. The C–O double bond character between atoms 1 and 2 would also diminish as atom 1 donates charge to the enolic hydrogen, and some double bond character would appear between atoms 4 and 5. This trend, which is found by Weinhold and Landis¹¹ in their discussion about the performance of the NRT indicator, is also found here with the distances of the two conformers, as illustrated in Table 5 for the optimized geometries at the BP86/Stuttgart ECP level of theory. Result for both bond order measures, calculated at BP86/def2-TZVPP level of theory are also displayed in Table 5. In this table can be seen that results for the NRT and for the fopBO are qualitatively similar, both suggesting the discussed trend. Quantitatively, the NRT indicator shows a more delocalized electronic structure for the closed conformation. It is interesting to note that the fopBO description at the current level of theory is actually closer to the NRT description presented in the text by Landis.

Cu,Zn Superoxide Dismutase Active Site. To assess the performance of the fopBO index for hydrogen bonds in a system within the atom-number range of commonly found on biologically oriented studies, we used a 91 atom reduced model of the active site of Cu,Zn SOD, built from a high resolution crystallographic structure.⁹ In that structure, which is shown in Figure 5, an aspartate residue is hydrogen-bonded to two histidine residues, one on each of its oxygens. These histidines are coordinated to the copper and to the zinc present in the active site of the enzyme, respectively.⁹ This aspartate residue is crucial for the functioning of the protein.⁴⁰ In the following discussion, hydrogen bonds are labeled as in Figure 5.

For the 91 atom model, we were unable to perform the NRT analysis to obtain the corresponding bond order indexes, as discussed in the Computational Details. Due to difficulties with the NBO program in working with high numbers of basis

Table 5. NRT-Based and fopBO Bond Order Indexes and Distances (in Å) for the Main Interactions in Open and Closed Conformations of β -Hydroxyacrolein, Based on a Calculation Performed at the BP86/def2-TZVPP Level of Theory

bond	open		closed		distance	
	NRT	fopBO	NRT	fopBO	open	closed
O1–C2	1.994	2.004	1.666	1.915	1.210	1.262
C2–C3	1.048	1.041	1.262	1.108	1.459	1.428
C3–C4	1.829	1.847	1.540	1.758	1.361	1.384
C4–O5	1.105	1.101	1.394	1.138	1.311	1.313
O5–H	0.989	0.994	0.925	0.921	0.972	1.060
H–O1	0.000	0.000	0.059	0.071	3.880	1.482

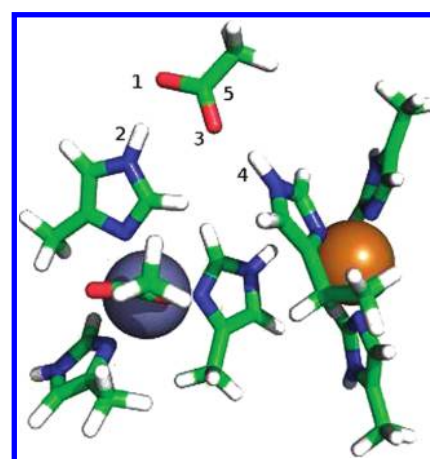


Figure 5. Reduced model of the active site of Cu,Zn SOD. Atoms involved in the hydrogen bonds in study are marked with numbers. Copper and zinc are shown as brown and gray spheres respectively, according to their AMBER⁴¹ radii.

functions, it was also impossible to obtain the fopBO indexes from calculations with the def2-TZVPP basis set. To solve this problem, carbon, zinc, and copper atoms were treated with Stuttgart ECPs while other atoms were treated at the def2-TZVPP level. The fopBO indexes and the bond distances are

given in Table 6. From this table it can be seen that fopBO indexes correctly correlate with the bond distances and angles assigning a greater bond order to the closest histidine.

Spin-Polarized Systems. *TEMPO Spin Label.* In order to assess the performance of NBO and fopBO indexes on spin polarized systems, we studied the well-known spin-label TEMPO (2,2,6,6-tetramethylpiperidine-1-oxyl radical). Again, in this case, the spin densities and the semioccupied Kohn–Sham orbital displayed in Figure 6 show that the unpaired electron is mostly localized in a N–O antibonding orbital. In agreement with this, the corresponding NRT and fopBO values, displayed in Table 7 show a double bond for the α spin–orbitals and a single bond for the β spin–orbitals. It can be seen that NRT and fopBO bond order give similar and correct values. The small differences found between the two measures can be attributed to the hyperconjugative effect of the vicinal methyl groups on the double bond, an effect especially suited for analysis with the fopBO approach.

Nitron–Hydroxyl Radical Spin-Adduct. In order to assess the performance of the fopBO index for a more delocalized system, we considered the spin-adduct between the hydroxyl radical and a spin trap with a nitron functional group. In this family of spin traps, the radical binds to a C–C double bond next to the N-oxide group. In the final adduct, the radical is localized in this N-oxide group. The geometry of the spin-adduct used in this work, a compound of biological interest,⁴² and the natural spin densities of this adduct are shown in Figure 7 and Figure 8, respectively. From the observation of Figure 8, it is clear that the semioccupied orbital corresponds to an antibonding orbital shared by the nitrogen and oxygen from one of the N-oxide groups. These atoms are marked with numbers 1 and 2, respectively, in Figure 7.

Table 6. Distances and fopBO Bond Order Indexes for Two Hydrogen Bonds in a Reduced Model of the Active Site of Cu, Zn SOD at Two Different Basis Sets^a

basis set	H-bond	distance O–H (Å)	fopBO
Stuttgart	O ₁ –H ₂	1.699	0.043
def2-TZVPP-Stuttgart	O ₁ –H ₂	1.699	0.044
Stuttgart	O ₃ –H ₄	1.738	0.037
def2-TZVPP-Stuttgart	O ₃ –H ₄	1.738	0.037

^a Numbers correspond to those used in Figure 5.

FopBO indexes for the N₁–O₂ interaction (numbers are according to those shown in Figure 7) in which the spin density is centered and the one for the C₃–O₄ bond on the interaction between the former hydroxyl radical and the nitron were calculated for the optimized structure of the spin-adduct and are shown in Table 8. With the standard configuration of NBO and the basis sets for this study (Stuttgart-ECP plus polarization functions and def2-TZVPP) we were not able to perform NRT analyses on the system.

From the examination of Table 8, it can be readily seen that there is no important difference among the α and β bond orders for the hydroxyl–carbon bond, and an important difference is noticed among the α and β spin–orbitals for the nitrogen–oxygen bond. For the latter, the β density shows a double bond (bond order close to 1, i.e., half of a double bond order) while for the α density the bond is single (bond order close to 0.5). This is compatible with the semioccupied orbital being mainly an antibonding orbital between the N and O atoms, which is the case for this system, as seen in Figure 8.

Hypervalent System. In order to test the performance of the fopBO index in a complex hypervalent system, we used the Li₄ molecule studied by Fuentealba and Savin.⁴³ In the mentioned work the authors conclude, based on an ELF²¹ analysis, that the Li–Li bonding in that system is of a 2e/3c type. On the basis of the structure optimized by Fuentealba and Savin, that can be seen in Figure 9, we calculated bond orders for the Li₄ molecule with the fopBO and the NRT measures, based on a single point calculation at B3LYP/def2-TZVPP level of theory. Although qualitatively correct, the results obtained for both NRT and fopBO measures were quantitatively not in agreement with the symmetry of the cluster. In order to further investigate this issue, we determined the values for both bond orders using four different basis sets: def2-SVP, def2-TZVPP, def2-QZVPP, and

Table 7. NRT-Based and fopBO Bond Order for the N–O Interaction in the TEMPO Interaction in α and β Spin-Orbitals, Calculated with a def2-TZVPP Basis Set

bond	α		β	
	NRT	fopBO	NRT	fopBO
O–N	0.520	0.522	1.001	1.012

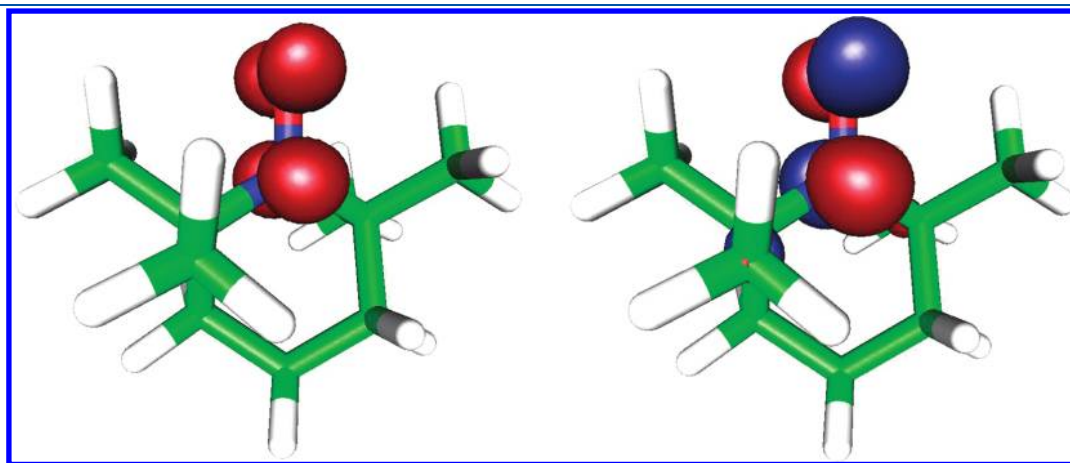


Figure 6. Spin densities (left) and semioccupied Kohn–Sham molecular orbital for the TEMPO spin-label, based on a B3LYP/def2-TZVPP calculation.

the Stuttgart relativistic ECP with its associated basis. The results can be seen in Table 9.

From the data displayed in Table 9, it can be seen that the treatment of the $\text{Li}_1\text{--Li}_2$ and $\text{Li}_1\text{--Li}_4$ interactions is basis-dependent. It can be also seen that the two methods, NRT and fopBO have trouble with different parts of the molecule: NRT gives the correct symmetry for the above-mentioned interaction already at the def2-TZVPP level, which is computationally affordable for most calculations. fopBO, on the other side, displays a significant error for these interactions at this level, which is, to the most part, corrected with the use of a def2-QZVPP basis set. This basis set is computationally too demanding for many practical applications. It is remarkable that the Stuttgart ECPs performs relatively well for fopBO, so its use, perhaps with additional polarization functions, could be helpful for problems of this kind.

Regarding to the $\text{Li}_2\text{--Li}_4$ interaction, both indexes yield the qualitatively correct result. The $\text{Li}_1\text{--Li}_4/\text{Li}_2\text{--Li}_4$ ratio is quantitatively better described by the NRT indicator.

This system is clearly one of the cases discussed in the Theoretical Basis. Because of the corrections being of a similar magnitude of the unperturbed structure, is not well treated by the

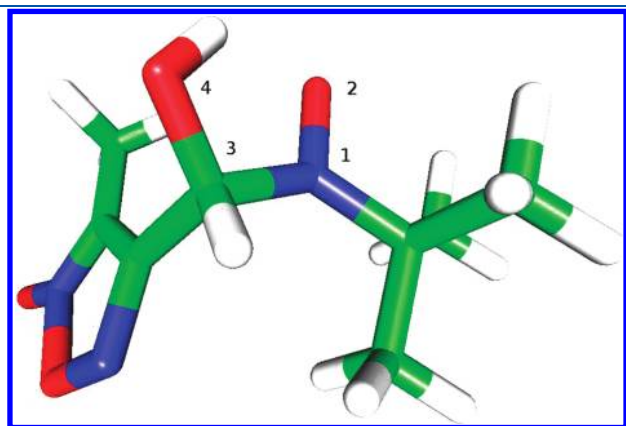


Figure 7. Optimized geometry of 2-methyl-*N*-((3-methyl-2-oxido-1,2,5-oxadiazol-4-yl)methylene)propan-2-amine oxide, reported by Porcal et al.⁴² bound to the hydroxyl radical. N and O atoms of interest for the present study, and the C and O atoms from the nitron group and the hydroxyl radical, respectively, are labeled with numbers 1, 2, 3, and 4 respectively.

perturbation-theory based fopBO. Despite this, the index still delivers values that lead to the same qualitative conclusions reached by Fuentealba and Savin. The fopBO index is thus not especially adequate for a specific set of systems, which are well-defined. This fact, added to its especial adequacy for systems with

Table 8. fopBO Bond Order Indexes for the Spin-Adduct Reported by Porcal et al.^{42 a}

bond	basis set	fopBO- α	fopBO- β
$\text{N}_1\text{--O}_2$	Stuttgart	0.514	1.001
$\text{N}_1\text{--O}_2$	def2-TZVPP	0.518	1.006
$\text{C}_3\text{--O}_4$	Stuttgart	0.512	0.512
$\text{C}_3\text{--O}_4$	def2-TZVPP	0.514	0.513

^a Bonds between the former hydroxyl radical and the spin-trap, and between the nitrogen and oxygen on the N-oxide group are shown at two different basis sets. Numbers correspond to those given in Figure 7.

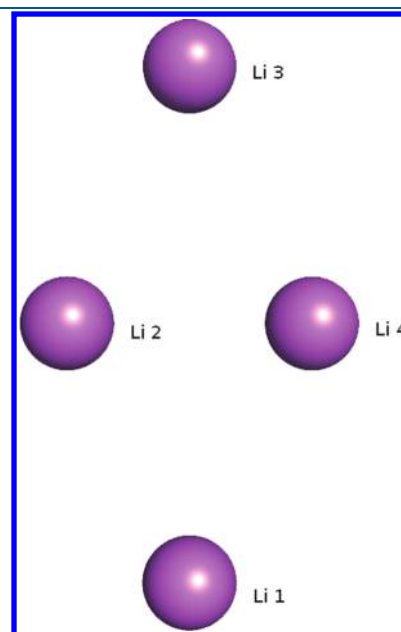


Figure 9. Geometry of the Li_4 molecule as reported by Fuentealba and Savin.⁴³

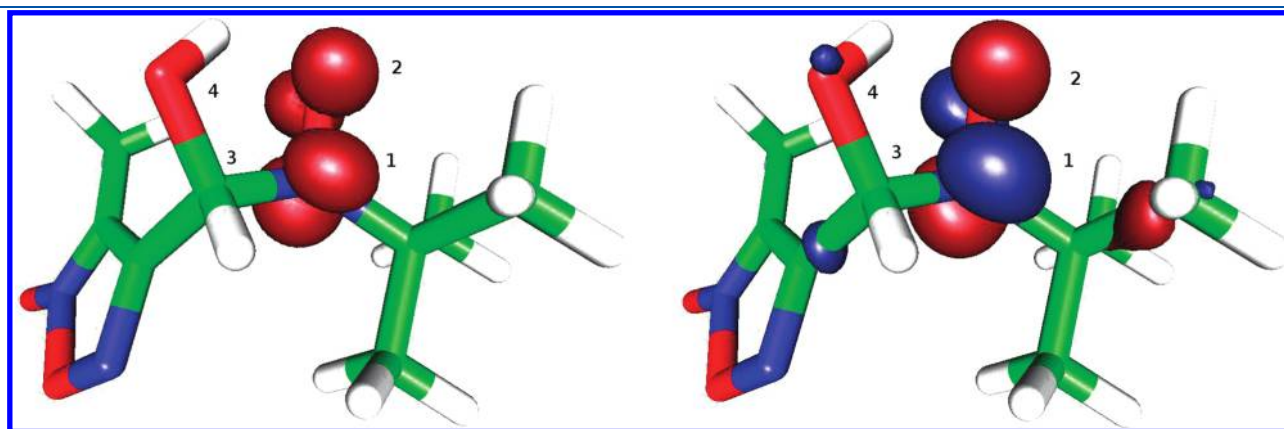


Figure 8. Spin densities (left) and semicupated Kohn–Sham molecular orbital for the 2-methyl-*N*-((3-methyl-2-oxido-1,2,5-oxadiazol-4-yl)methylene)propan-2-amine oxide reported by Porcal et al.,⁴² bound to the hydroxyl radical, based on a B3LYP/def2-TZVPP calculation.

Table 9. NRT and fopBO Bond Orders for Li–Li Interactions in the Li₄ Structure As Obtained by Fuentealb and Savin^{43 a}

basis set	Li ₁ –Li ₂ (3.01 Å)		Li ₁ –Li ₄ (3.01 Å)		Li ₂ –Li ₄ (2.58 Å)	
	NRT	fopBO	NRT	fopBO	NRT	fopBO
Stuttgart	0.288	0.492	0.314	0.421	0.337	0.843
def2-SVP	0.308	0.380	0.317	0.546	0.357	1.091
def2-TZVPP	0.310	0.420	0.310	0.504	0.361	1.008
def2-QZVPP	0.313	0.452	0.308	0.476	0.358	0.953

^a Numbers correspond to those given in Figure 9.

a large number of electrons and the description of weak interactions highlights the complementary nature of this measure and the NRT-based index.

CONCLUDING REMARKS

In this work, a bond order index inscribed into the natural bond orbital framework has been presented. The stability upon basis set change of this bond order index has been shown to be comparable to that of the natural resonance theory-based bond order traditionally used for NBO analysis. Although in most cases the results yielded by both bond order indexes are similar, when differences occur, comparison of both measures appears to be useful to understand the nature of the interaction. Considering this, we recommend that both bond orders be calculated should the size of the system allows so.

The most important advantage of the fopBO index when compared to the NRT-based measure is the possibility of studying molecules with a large number of atoms, which is the case of most biologically interesting systems. This work shows that systems for which the NRT analysis and associate bond order index are not possible to calculate, can be analyzed with the fopBO measure. Hence the number of systems that can be thoughtfully studied with NBO analysis is increased.

In addition, since the fopBO is calculated with the same values used to obtain the second-order perturbation theory interaction energies in the standard NBO analysis,⁵ its results can be readily rationalized in terms of those energies, and contribution of different interactions can be identified.

The fopBO bond order measure is, thus, an easy to calculate and well behaving index, especially suited for its use along with the NBO analysis tools.¹²

ACKNOWLEDGMENT

P.F. and F.M. express thanks for the support from Financiamiento Basal para centros científicos y tecnológicos de excelencia, CONICYT, FB0807 (CEDENNA). P.F. thanks Fondecyt for support through Grant 1080184. F.M. thanks Fondecyt for support through grant 1100162. S.M.-R. and R.M.-A. each thank CONICYT for a Ph.D. studies scholarship. R.M.-A. thanks BECAS CHILE for a research stay scholarship and Prof. Pekka Pyykkö and Dr. Ville Kaila for useful discussions.

REFERENCES

- Becke, A. D.; Edgecombe, K. E. *J. Chem. Phys.* **1990**, *92*, 5397–5403.
- Savin, A.; Nesper, R.; Wengert, S.; Fässler, T. F. *Angew Chem Int Ed* **2003**, *36*, 1808–1832.

- Bader, R. W. *Atoms in Molecules: A Quantum Theory*, 1st ed.; Oxford University Press: Oxford, U.K., 1990.
- Foster, J. P.; Weinhold, F. *J. Am. Chem. Soc.* **1980**, *102*, 7211–7218.
- Weinhold, F. In *Encyclopedia of Computational Chemistry*; Schleyer, P. v. R., Allinger, N. L., Clark, T., Gasteiger, J., Kollman, P. A., Schaefer, H. F., III, Schreiner, P. R., Eds.; John Wiley and Sons: New York, 1998; pp 1792–1811.
- Mayer, I. *J. C. Chem.* **2006**, *28*, 204–221.
- (a) Glendening, E. D.; Weinhold, F. *J. Comput. Chem.* **1998**, *19*, 593–609. (b) Glendening, E. D.; Weinhold, F. *J. Comput. Chem.* **1998**, *19*, 610–627. (c) Glendening, E. D.; Badenhoop, J. K.; Weinhold, F. *J. Comput. Chem.* **1998**, *19*, 628–646.
- Hough, M. A.; Hasnain, S. S. *J. Biol. Mol.* **1999**, *287*, 579–592.
- Hough, M. A.; Hasnain, S. S. *Structure* **2003**, *11*, 937–946.
- Cudkovicz, M. E.; McKenna-Yasek, T. D.; Sapp, P. E.; Chin, W.; Geller, B.; Hayden, D. L.; Schoenfeld, D. A.; Hosler, B. A.; Horvitz, H.; Brown, R. H. *Ann. Neurol.* **1997**, *41*, 210.
- Weinhold, F.; Landis, C. *Valency and Bonding: A Natural Bond Orbital Donor-Acceptor Perspective*, 1st ed.; Cambridge University Press: Chichester, U.K., 2005.
- Glendening, E. D.; Badenhoop, J. K.; Reed, A. E.; Carpenter, J. E.; Bohmann, J. A.; Morales, C. M.; Weinhold, F. *NBO 5.0*, 2001.
- NBO References and Bibliography*. <http://www.chem.wisc.edu/~nbo5/biblio.htm>.
- Reed, A. E.; Curtis, L. A.; Weinhold, F. *Chem Rev* **1988**, *88*, 899–926.
- Stewart, J. P. *J. Mol. Model* **2007**, *13*, 1173–2113.
- Stewart, J. P. *The MOPAC2009 Program*. <http://openmopac.net/MOPAC2009.html>.
- Becke, A. D. *Phys. Rev. A* **1988**, *38*, 3098–3100.
- Perdew, J. J. *Phys. Rev. B* **1986**, *33*, 8822–8824.
- Bergner, A.; Dolg, M.; Küchle, W.; Stoll, H.; Preuß, H. *Mol. Phys.* **1993**, *80*, 1431–1441.
- Gaussian basis sets for chemical calculations*, 1st ed.; Huzinaga, S., Ed.; Elsevier Science Publishers B.V.: Amsterdam, The Netherlands, 1984.
- Ahlrichs, R.; Bär, M.; Häser, M.; Horn, H.; Kölmel, C. *Chem. Phys. Lett.* **1989**, *162*, 165–169.
- Eichkorn, K.; Treutler, O.; Oehm, H.; Häser, M.; Ahlrichs, R. *Chem. Phys. Lett.* **1995**, *242*, 652–660.
- Treutler, O.; Ahlrichs, R. *J. Chem. Phys.* **1995**, *102*, 346–355.
- Eichkorn, K.; Weigend, F.; Treutler, O.; Ahlrichs, R. *Theor. Chem. Acc.* **1997**, *97*, 119–124.
- Weigend, F. *Phys. Chem. Chem. Phys.* **2002**, *4*, 4285–4291.
- Ahlrichs, R. *Phys. Chem. Chem. Phys.* **2004**, *6*, 5119–5121.
- The Avogadro Molecular Editor*. http://avogadro.openmolecules.net/wiki/Main_Page.
- Becke, A. D. *J. Chem. Phys.* **1993**, *98*, 5648–5652.
- Lee, C.; Yang, W.; Parr, R. G. *Phys. Rev. B* **1988**, *37*, 785–789.
- Vosko, S. H.; Wilk, L.; Nusair, M. *Can. J. Phys.* **1980**, *58*, 1200–1211.
- Stevens, P. J.; Devlin, F. J.; Chabalowski, C. F.; Frisch, M. J. *J. Phys. Chem.* **1994**, *98*, 11623–11627.
- Granovsky, A. A. *Firefly version 7.1.F*. <http://classic.chem.msu.su/gran/gamess/index.html>.
- Schmidt, M. W.; Baldridge, K. K.; Boatz, J. A.; Elbert, S. T.; Gordon, M. S.; Jensen, J. H.; Koseki, S.; Matsunaga, N.; Nguyen, K. A.; Su, S.; Windus, T. L.; Dupuis, M., Jr.; Montgomery, J. A. *J. Comput. Chem.* **1992**, *14*, 1347–1363.
- Binkley, J. S.; Pople, J. A.; J., H. W. *J. Am. Chem. Soc.* **1980**, *102*, 939–947.
- Hehre, W. J.; Radom, L.; Schleyer, P. V.; Pople, J. A. *AB INITIO Molecular Orbital Theory*, 1st ed.; Wiley-Interscience: New York, 1986.
- Weigend, F.; Ahlrichs, R. *Phys. Chem. Chem. Phys.* **2005**, *7*, 3297–3305.
- Schrödinger, L. L. C. *The PyMOL Molecular Graphics System, Version 1.3r1*, 2010.

- (38) Laaksonen, L. *J. Mol. Graphics* **1992**, *10*, 33–34.
- (39) Bergman, L.; Laaksonen, L.; Laaksonen, A. *J. Mol. Graphics* **1997**, *15*, 301–306.
- (40) Banci, L.; Bertini, I.; Cabelli, D. E.; Hellewell, R. A.; Tung, J. W.; Viezzoli, M. S. *Eur. J. Biochem.* **1991**, *196*, 123–128.
- (41) Ponder, J. W.; Case, D. A. *Adv. Protein Chem.* **2003**, *66*, 27–85.
- (42) Porcal, W.; Hernandez, P.; Gonzalez, M.; Ferreira, A.; Olea-Azar, C.; Cerecetto, H.; Castro, A. *J. Med. Chem.* **2008**, *51*, 6150–6159.
- (43) Fuentealba, P.; Savin, A. *J. Phys. Chem. A* **2001**, *105*, 11531–11533.